JMEPEG (2012) 21:877–881
DOI: 10.1007/s11665-011-9959-3

1059-9495/$19.00

Dilithium dialuminium trisilicate Crystalline Phase Prepared from Coal Fly Ash

Zhitong Yao, Meisheng Xia, and Ying Ye

(Submitted June 30, 2010; in revised form April 9, 2011)

The dilithium dialuminium trisilicate phase $Li_2Al_2Si_3O_{10}$ was prepared using coal fly ash and lithium hydroxide monohydrate $LiOH·H_2O$ as precursors. The influences of various preparation conditions on $Li_2Al_2Si_3O_{10}$ forming were investigated. The results showed that the optimum additive amount of $LiOH·H_2O$ was about 20%. The onset of calcining temperature and time was identified as 980 °C and 1 h, respectively. XRD analysis indicated that the content of $Li_2Al_2Si_3O_{10}$ phase increased at the expense of quartz and mullite, with calcining temperatures increasing and time extending. SEM observation revealed that the calcined samples were drastically interlocked together with the prolonging of time. The obtained $Li_2Al_2Si_3O_{10}$ phase was well crystallized and with small grain size.

Keywords coal fly ash, dilithium dialuminium trisilicate, lithium glass-ceramic, lithium hydroxide monohydrate

1. Introduction

Coal fly ash is a by-product derived from the coal combustion in thermoelectric plants. Approximate 500 million tonnes of ash is discharged annually throughout the world (Ref 1, 2). It must be reduced prior to disposal. Accordingly, efforts have been made to find alternative uses for coal fly ash. For instance, about 20% ash has been used as a pozzolanic material in concrete applications (Ref 3, 4). It has also been used in road-based construction, soil amendment, and as filler in plastic composite materials (Ref 5, 6). However, the utilization rate of coal fly ash in these applications is far less than that of ash being generated. The remainder is directly discharged, which may cause long-term adverse environmental effects. It is imperative to develop new recycling techniques for coal fly ash.

As is well known, the coal fly ash contains appreciable amounts of SiO_2, Al_2O_3, CaO, Fe_2O_3, among other oxides (Ref 7). These oxides have been mainly considered as a low cost material for ceramic industry. In addition, the fine powder form makes it suitable to be directly incorporated into ceramic pastes with almost no pretreatment (Ref 7). Recent research has investigated the production of glass, glass-ceramic, or sintered materials prepared from coal fly ash (e.g., Ref 7, 8). Due to their low or negative coefficient of thermal expansion (CTE), glass-ceramics materials based on Li_2O-Al_2O_3-SiO_2 ternary system have important industrial applications. For instance, dilithium dialuminium trisilicate ($Li_2Al_2Si_3O_{10}$) phase has been used as materials for telescope mirrors, kitchen stove hot plate and heat-resistant ware, hybrid circuit substrates, etc. (Ref 9, 10). However, these materials are usually prepared by high-grade reagents (Ref 11, 12), causing the product to be very expensive. Recently, there has been report on preparation of $Li_2Al_2Si_3O_{10}$ phase using bottom ash (Ref 10). The use of coal fly ash as starting material has not been described in the literature. Therefore, in this study, we attempt to prepare of $Li_2Al_2Si_3O_{10}$ phase using coal fly ash and lithium hydroxide monohydrate ($LiOH·H_2O$) as precursors. The additive amount of $LiOH·H_2O$, calcining temperatures, and time was investigated to find out the optimum preparation conditions. The calcined samples were identified by x-ray diffraction (XRD) and characterized by scanning electron microscopy (SEM), Fourier transform infrared spectroscopy (FT-IR) analysis as well.

Zhitong Yao, Department of Ocean Science and Engineering, Zhejiang University, Hangzhou 310058, China; and School of Environment, Tsinghua University, Beijing 100084, China; and **Meisheng Xia** and **Ying Ye**, Department of Ocean Science and Engineering, Zhejiang University, Hangzhou 310058, China; Contact e-mail: gsyeying@zju.edu.cn.

2. Experimental Procedure

2.1 Starting Materials

The coal fly ash used in this study was collected from Hangzhou thermal power plant in China. Its chemical composition consists of the following oxides (in wt.%): SiO_2 50.5, Al_2O_3 35.9, Fe_2O_3 5.3, CaO 4.6, TiO_2 1.5, K_2O 1.3, and other compounds 0.9. XRD analysis indicates that its major phases are mullite (JCPDS card no. 15-776) and quartz (JCPDS card no. 5-490), together with amorphous components mainly based on aluminosilicate glass.

2.2 Pretreatment

It was reported that the magnetite content in ash influences the $Li_2Al_2Si_3O_{10}$ properties. High content causes poor properties, otherwise they improve (Ref 10, 13). Magnetic separation is an efficient approach for iron removal and thus used in this study. The process was performed on WCF-2 multi-purpose magnetic analytical meter (Beijing Geological Instrument Factory, Beijing, China) with a constant magnetic current of 2.8 A.

2.3 Preparation of $Li_2Al_2Si_3O_{10}$

The pretreated coal fly ash was mixed and ground with different amounts (10, 15, 20, and 25%) of $LiOH \cdot H_2O$ powders to obtain a homogeneous mixture. Then, the mixture was put into a crucible and heated at 980 °C for 1 h. With the goal of optimizing the process, three calcining temperatures (950, 980, and 1000 °C) and calcining time extended from 15 min to 6 h were selected.

2.4 Measurements

The coal fly ash samples were ground and analyzed by means of x-ray diffraction to determine the crystalline phases present. A Rigaku Denki diffractometer (model D/max-IIB) was operated at 40 kV and 30 mA, with Cu Kα as the radiation source. The detector was scanned in the range of 10-80° (2θ) and at a step scan of 0.02°. Scanning electron microscopy investigations were conducted in a Hitachi S-4800 scanning electron microscope (back-scattered electron mode) to observe the morphology of the samples. Transmission IR spectra was recorded by a Nicolet Nexus-670 Fourier transform infrared spectrometer with a resolution of 2 cm^{-1} and using the KBr disk method. The thermal expansion coefficient of the specimen was measured using a dilatometer (DIL402C, Netzsch, Germany).

3. Results

3.1 Influence of $LiOH \cdot H_2O$ Addition

Figure 1 depicts the XRD patterns of coal fly ash samples calcined with different amounts of $LiOH \cdot H_2O$ (10, 15, 20, and 25%) at 980 °C for 1 h. It showed that the major crystalline phases of the sample calcined with 10% $LiOH \cdot H_2O$ were lithium aluminum silicate ($Li_2Al_2Si_3O_{10}$, JCPDS card no. 25-1183) and low-quartz solid solution (JCPDS card no. 65-466), with little mullite detected. Further increase in $LiOH \cdot H_2O$ addition, the color of samples changed from yellowish to reddish. The content of $Li_2Al_2Si_3O_{10}$ phase increased at the expense of mullite and quartz. It may result from the gradual incorporation of mullite and quartz with Li released from $LiOH \cdot H_2O$. The chemical reaction equations involved in these processes can be described as follows (Eq 1 and 2):

$$2LiOH \cdot H_2O \rightarrow Li_2O + 3H_2O \quad \text{(Eq 1)}$$

$$3SiO_2 + Li_2O + Al_2O_3 \rightarrow Li_2Al_2Si_3O_{10} \quad \text{(Eq 2)}$$

When the additive amount of $LiOH \cdot H_2O$ increased up to 20%, the pink color of the sample increased. The crystalline phase manifested as $Li_2Al_2Si_3O_{10}$. It indicated that the mullite and quartz phases were well incorporated and the optimum amount of $LiOH \cdot H_2O$ was about 20%.

3.2 Influence of Calcining Temperatures

Figure 2 displays the XRD patterns of samples calcined with 20% $LiOH \cdot H_2O$ at different temperatures (950, 980, and 1000 °C) for 1 h. It revealed that the major phases present in the sample calcined at 950 °C was $Li_2Al_2Si_3O_{10}$, with little quartz appeared. The content of quartz reduced with an increase of calcining temperature. On the contrary, more $Li_2Al_2Si_3O_{10}$ phase occurred. When the calcining temperature increased up to 980 °C, the sample was almost completely transformed to $Li_2Al_2Si_3O_{10}$. However, there was no significant difference in phases when the calcining temperature was up to 1000 °C. This indicated that the onset temperature for $Li_2Al_2Si_3O_{10}$ forming was about 980 °C.

3.3 Influence of Calcining Time

The XRD patterns of samples calcined for different times are illustrated in Fig. 3. It can be seen that the major phases of the sample calcined for 15 min are $Li_2Al_2Si_3O_{10}$ and $LiAlSiO_4$ (JCPDS card no. 26-839) with little quartz (JCPDS card no. 87-2096). When the calcining time prolonged to 30 min, the color of the sample increased, but still maintained yellowish.

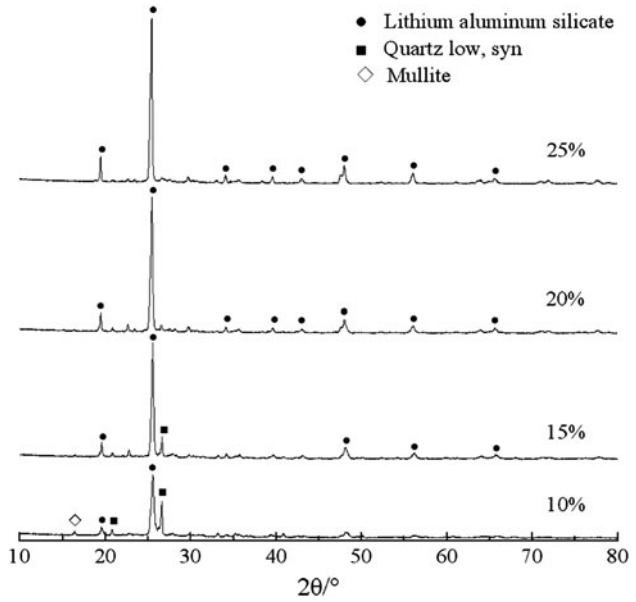

Fig. 1 XRD patterns of fly ash samples calcined with different amounts of $LiOH \cdot H_2O$ at 980 °C for 1 h

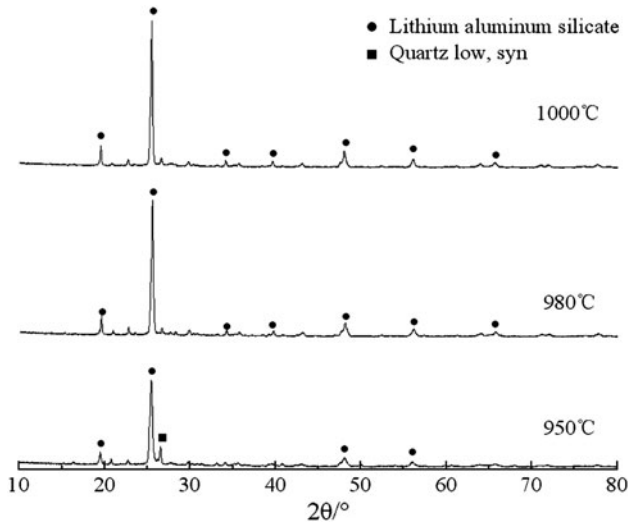

Fig. 2 XRD patterns of fly ash samples calcined with 20% $LiOH \cdot H_2O$ at different temperatures for 1 h

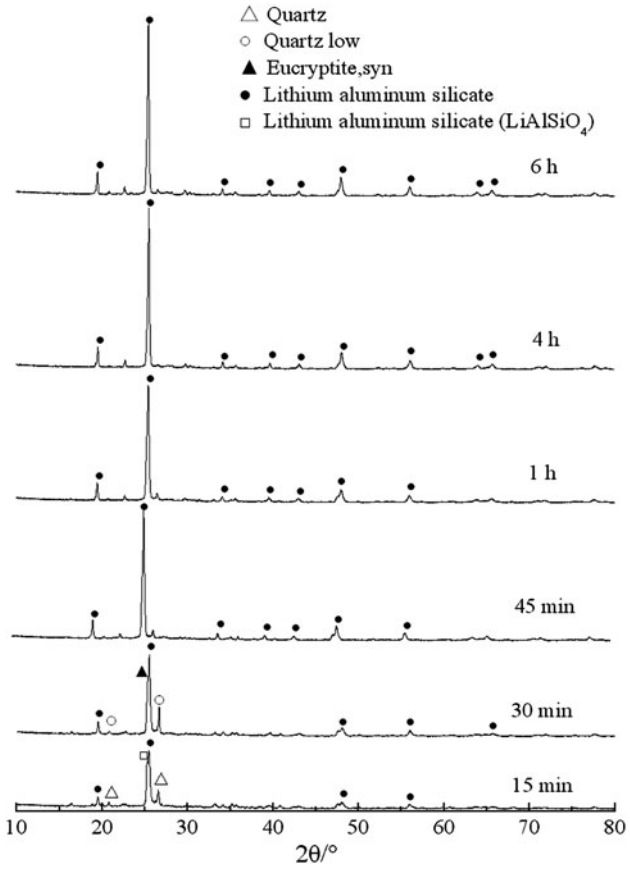

Fig. 3 XRD patterns of fly ash samples calcined with 20% $LiOH{\cdot}H_2O$ at 980 °C for different times

The eucryptite phase ($LiAlSiO_4$, JCPDS card no. 75-2330) was detected in the sample, which indicated partial calcining degree. Further increasing the time to more than 1 h, it can be seen that the sample transformed to $Li_2Al_2Si_3O_{10}$ phase. In addition, the color of the samples changed to reddish or pink, indicating a higher calcining degree. The optimum calcining time for fly ash was identified as 1 h.

Thereafter, SEM investigations were conducted to investigate the particle morphology and surface microstructural evolution of the samples. For a comparison, the SEM image of raw fly ash was also included in Fig. 4. The coal fly ash without calcining was characterized by spherically and irregularly round shaped. The interlocked needle-like mullite crystals were also observed on the external surface of ash particle. With the extending of calcining time, the round-shaped particle gradually reduced. Simultaneously, particles substantially interlocked together and formed agglomeration. As the major phases of samples calcined for 45 min and 1 h were both $Li_2Al_2Si_3O_{10}$ (shown in Fig. 3), we observed the surface morphology and found that the smaller grain size and compacted microstructure developed as a result of prolonged calcining time.

3.4 FT-IR Results

From the above results, we can see that the $Li_2Al_2Si_3O_{10}$ phase could be obtained under the optimum condition of calcining coal fly ash with 20% $Li(OH){\cdot}H_2O$ at 980 °C for 1 h. In order to clarify its crystallization behavior, FT-IR experiments were undertaken on the parent coal fly ash and calcined sample. In Fig. 5, the absorption peak located at 1100-800 cm^{-1} belonged to the asymmetric stretching vibration of

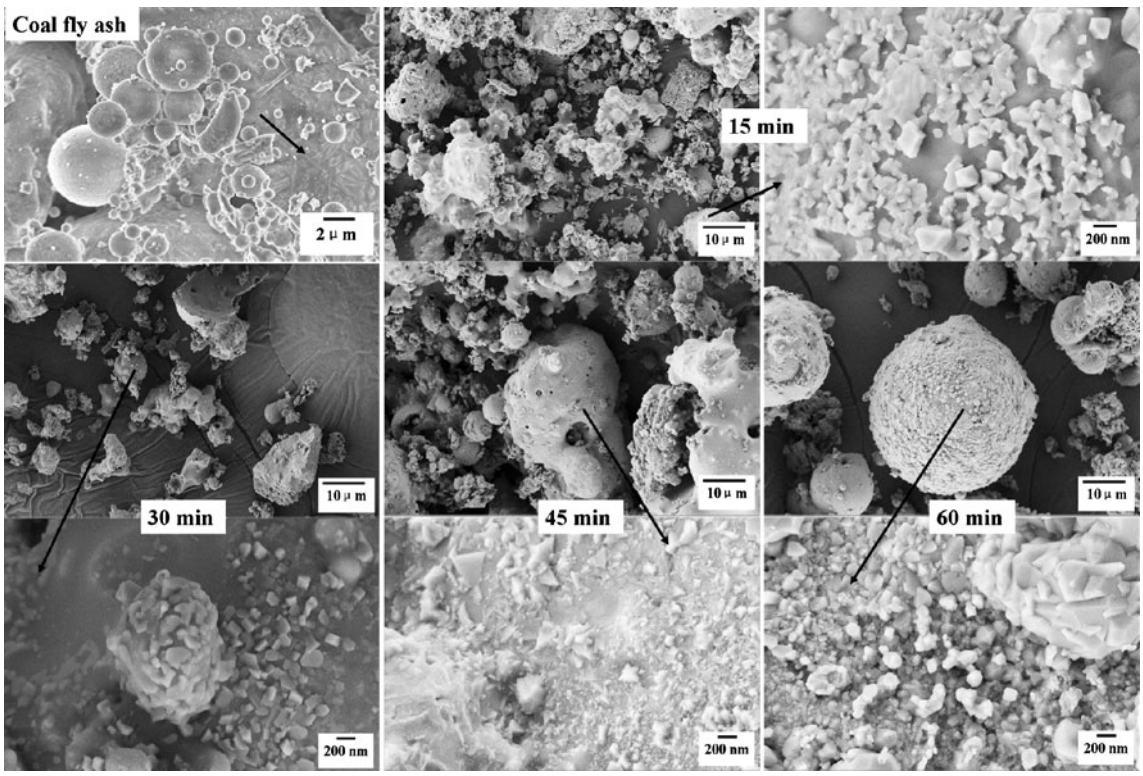

Fig. 4 SEM images of fly ash samples calcined with 20% $LiOH{\cdot}H_2O$ at 980 °C for different times

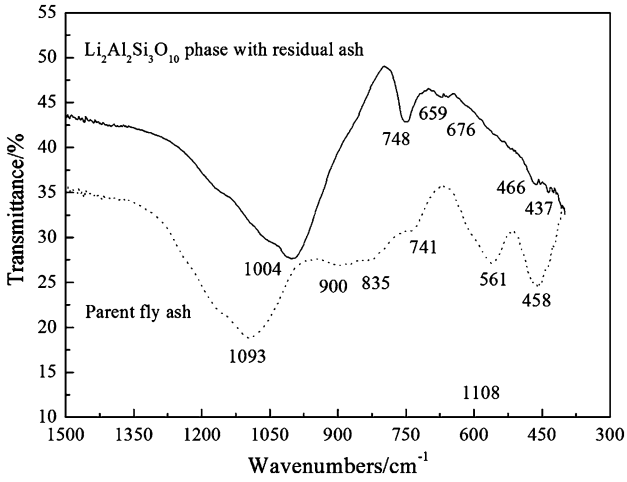

Fig. 5 FT-IR spectra of parent fly ash and calcined sample

Si-O-Si within [SiO_4]. The band 750-550 cm^{-1} was assigned to Si-O-Si symmetric stretching vibration between the tetrahedrons. While, the band 500-400 cm^{-1} was due to bending vibration of Si-O-Si and Si-O-Al linkage (Ref 14, 15). It was observed that the spectrum of calcined sample ($Li_2Al_2Si_3O_{10}$ phase with residual ash) showed a negative shift of the Si-O-Si asymmetric stretching, which highlighted a decrease in the polymerization degree of [SiO_4] tetrahedrons and a rearrangement of the silica network (Ref 14, 16).

4. Discussions

The iron oxides content in starting material have a negative effect on the thermal expansion coefficient of product (Ref 17, 18), so it is important to reduce the iron oxides content before processing. In this study, the coal fly ash was pretreated with magnetic separation method for iron removal. After magnetic separation, the contents of three main components SiO_2, Al_2O_3, and Fe_2O_3 in raw fly ash were 53.6, 36.1, and 1.5%, respectively. The recovery of Fe_2O_3 reached by 71.6% and the capture efficiency (the mass ratio of the magnetic fraction to starting samples) was 31.9%.

Through a series of experiments, the $Li_2Al_2Si_3O_{10}$ phase could be obtained under the optimum condition of calcining ash with 20% Li(OH)·H_2O at 980 °C for 1 h. SEM observations revealed that it presented smaller grain size and compacted microstructure. The measured CTE of calcined sample ($Li_2Al_2Si_3O_{10}$ phase with residual ash) was -2.16×10^{-6}/°C in the temperature range 25-300 °C. This is smaller than that for the commercial lithium glass-ceramics (-2.34×10^7 °C^{-1} to 50×10^7 °C^{-1}) (Ref 9). It is worth mentioning that, although additional nucleate agents were not added in the preparation process, the ash samples contained appreciable amount of TiO_2 and Al_2O_3, which may act as nucleate agent and glass-former, respectively. Calcinations at 980 °C for 1 h in the process were aimed to liberate the lithium hydroxide monohydrate and obtain the vitreous phase. The calcining temperature and time was relative low and short, which may be due to the low decomposed temperature for lithium hydroxide monohydrate.

5. Conclusions

From the experimental results, the following conclusions can be drawn:

(1) The $Li_2Al_2Si_3O_{10}$ phase was obtained using coal fly ash after magnetic separation pretreatment as the precursor. The optimum calcining conditions were identified as 980 °C calcined with 20% LiOH·H_2O for 1 h.
(2) XRD analysis indicated that the content of $Li_2Al_2Si_3O_{10}$ phase was gradually increased by simultaneously consuming quartz and mullite with an increase of calcining temperatures and time. The color of the samples changed from yellowish to pink as the calcining time extended from 15 min to 6 h, indicating the different sintering degrees.
(3) SEM observation showed that the coal fly ash samples were drastically interlocked together and developed a well-calcined microstructure.
(4) The FT-IR analysis of the calcined sample ($Li_2Al_2Si_3O_{10}$ phase with residual ash) indicated a decrease in the polymerization degree of [SiO_4] tetrahedrons and a rearrangement of the silica network.

Acknowledgments

This study was financially supported by the Chinese National 863 High Technology (Grant no. 2007AA06Z128) and Fundamental Research Funds for the Central Universities.

References

1. C.F. Wang, J.S. Li, L.J. Wang, and X.Y. Sun, Influence of NaOH Concentrations on Synthesis of Pure-Form Zeolite A from Fly Ash Using Two-Stage Method, *J. Hazard. Mater.*, 2008, **155**, p 58–64
2. V.S. Ramachandran, *Concrete Admixtures Handbook: Properties, Science, and Technology*, 2nd ed., William Andrew Publishing, Norwich, 1995
3. M. Inada, Y. Eguchi, N. Enomoto, and J. Hojo, Synthesis of Zeolite From Coal Fly Ashes with Different Silica-Alumina Composition, *Fuel*, 2005, **84**, p 299–304
4. V. Aggarwal, S.M. Gupta, and S.N. Sachdeva, Concrete Durability Through High Volume Fly Ash Concrete (HVFC) a Literature Review, *Int. J. Eng. Sci. Technol.*, 2010, **2**, p 4473–4477
5. H. Cho, D. Oh, and K. Kim, A Study on Removal Characteristics of Heavy Metals from Aqueous Solution by Fly Ash, *J. Hazard. Mater. B*, 2005, **127**, p 187–195
6. M. Ilic, C. Cheeseman, C. Sollars, and J. Knight, Mineralogy and Microstructure of Sintered Lignite Coal Fly Ash, *Fuel*, 2003, **82**, p 331–336
7. M. Erol, S. Kuüçükbayrak, and A. Ersoy-Meriçboyu, Characterization of Sintered Coal Fly Ashes, *Fuel*, 2008, **87**, p 1334–1340
8. L. Barbieri, I. Lancellotti, T. Manfredini, I. Queralt, J.M. Rincon, and M. Romero, Design Obtainment and Properties of Glasses and Sintered Materials from Coal Fly Ash, *Fuel*, 1999, **78**, p 271–276
9. Z. Strnad, Glass-Ceramic Materials, Glass Science and Technology, Vol 8, Elsevier, New York, 1986, p 76–96, 195–199
10. C.T. Kniess, J.C. De Lima, P.B. Prates, N.C. Kuhnen, and H.G. Riella, Dilithium Dialuminium Trisilicate Phase Obtained Using Coal Bottom Ash, *J. Non-Cryst. Solids*, 2007, **353**, p 4819–4822
11. Y. Li, Q.H. Wei, L. Li, C.H. Wang, X.L. Zhang, and F. Gao, Effects of Heat-Treatment Temperature on the Properties of Negative CTE Eucryptite Ceramics, *Adv. Mater. Res.*, 2010, **105–106**, p 123–125

12. S.M. Wang, F.H. Kuang, Q.Z. Yan, Y.C. Zhang, and C.C. Ge, Crystallization Behavior of a New Transparent Glass-Ceramics, *Adv. Mater. Res.*, 2010, **105–106**, p 597–599
13. C.T. Kniess, N.C. Kuhnen, H.G. Riella, E. Neves, and C.D.G. de Borba, Study of Iron Oxide Quantity on Bottom Ashes from Mineral Coal to Glass Ceramic Production, *Quim. Nova*, 2002, **25**, p 926–930
14. P. Pisciella and M. Pelino, Thermal Expansion Investigation of Iron Rich Sintered Material, *J. Eur. Ceram. Soc.*, 2008, **28**, p 3021–3026
15. M.S. Ma, W. Ni, Y.L. Wang, Z.J. Wang, and F.M. Liu, The Effect of TiO_2 on Phase Separation and Crystallization of Glass-Ceramics in CaO-MgO-Al_2O_3-SiO_2-Na_2O System, *J. Non-Cryst. Solids*, 2008, **354**, p 5395–5401
16. P.R. Foy, *Fabrication and Characterization of Calcium Aluminate Glass Fibers*, Rutgers, The State University of New Jersey, New Brunswick, 2008, p 16
17. S.B. Qadri, C. Fahed, H. Kim, A. Pique, N.A. Mahadik, and M.V. Rao, Thermal Expansion Studies of Indium-Iron Oxide, *Phys. Status Solidi B*, 2011, **248**, p 928–930
18. S.M. Wang, Effects of Fe on Crystallization and Properties of a New High Infrared Radiance Glass-Ceramics, *Environ. Sci. Technol.*, 2010, **44**(12), p 4816–4820